ELSEVIER

Nuclear Instruments and Methods in Physics Research B 164–165 (2000) 310–317

NIM B
Beam Interactions with Materials & Atoms

www.elsevier.nl/locate/nimb

Exit angle, energy loss and internuclear distance distributions of H_2^+ ions dissociated when traversing different materials

Rafael Garcia-Molina [a,*], Isabel Abril [b], Cristian D. Denton [a,c], Néstor R. Arista [c]

[a] *Departamento de Física, Universidad de Murcia, Apartado 4021, E-30080 Murcia, Spain*
[b] *Departament de Física Aplicada, Universitat d'Alacant, Apartat 99, E-03080 Alacant, Spain*
[c] *Instituto Balseiro, Centro Atómico Bariloche, RA-8400 Bariloche, Argentina*

Abstract

We have performed computer simulations of the trajectory followed by each proton resulting from the dissociation of H_2^+ molecules when traversing a thin solid target. We use the dielectric formalism to describe the forces due to electronic excitations in the medium, and we also consider the Coulomb repulsion between the pair of protons. Nuclear collisions with target nuclei are incorporated through a Monte Carlo code and the effect of the coherent scattering is taken into account by means of an effective force model. The distributions of exit angle, energy loss and internuclear separations of the protons fragments are discussed for the case of amorphous carbon and aluminum targets.

1. Introduction

When a hydrogen molecular ion bombards a solid it is fragmented into its constituents, which travel in correlated motion inside the target. Many interesting phenomena and applications are related to the manner in which energy is deposited in the solid by these correlated protons, which is different from the energy deposited when the same protons are uncorrelated [1,2]. Some of these differences can be described in terms of the wake potential [3,4] accompanying a charged projectile inside a solid, in such a manner that each proton not only feels its self-induced retarding force, but also the wake force produced by its partner proton. Several works have been devoted to study the consequences of this so-called *vicinage effect* in the motion of the correlated protons resulting from the dissociation of molecular ions, as compared to the case of single protons [1,5–11].

The purpose of this work is to analyze the distributions in exit angle, energy loss and internuclear distances of the protons resulting from the dissociation of fast H_2^+ molecular ions when traversing targets of different materials, such as amorphous carbon and aluminum.

The organization of this paper is the following: in Section 2 we present briefly the basis of our computer simulations, whose results are discussed in Section 3; finally, a summary and the conclusions are presented in Section 4.

* Corresponding author.
E-mail address: rgm@um.es (R. Garcia-Molina).

0168-583X/00/$ - see front matter
PII: S0168-583X(99)01177-5

2. Model

When a fast H_2^+ ion enters a solid, its binding electron is stripped off in the first atomic layers; this results in the motion through the solid of two protons in a correlated way. We have done a computer simulation that follows in a realistic manner the motion of these protons, whose coordinates and velocities are obtained as a function of the time. Then it is possible to know the exit angle and the relative position of the proton fragments when they leave the target, and the energy spectrum when reaching the detector.

Before entering the target, the H_2^+ ion is characterised by two parameters: the initial internuclear distance d_0 and the angle β between the internuclear vector and the initial direction of motion. In our simulations these parameters are chosen trying to reproduce standard experimental situations. The angle β is randomly distributed and the distance d_0 is chosen according to the population of vibrational states of the H_2^+ molecule [1,12,13]. After the dissociation of the H_2^+ ion, each of the two protons is subjected to the following interactions during their motion inside the stopping medium: (i) the self-retarding force (usually known as stopping power) due to the electric potential induced in the medium by its passage, (ii) the interference force induced in the medium by its partner proton, (iii) the Coulomb repulsion with its partner, and (iv) the nuclear collisions with the target atoms. With these ingredients, the positions and velocities of both protons are calculated at each time step solving numerically their coupled equations of motion. In the following, atomic units are used, except when otherwise stated.

The dielectric formalism [4] was used to describe the self-retarding and the interference forces; fluctuations in the electronic energy loss were also taken into account choosing the self-retarding force from a gaussian distribution centred in the stopping power corresponding to the instantaneous velocity of the proton, and with a width related to the energy loss straggling. Moreover, as each proton slows down along its trajectory, the velocity dependence of the corresponding self-retarding force is also taken into account. The properties of the stopping medium are contained in its energy loss function, which is properly described [4,14] through a fitting of available experimental data by a linear combination of Mermin-type [15] energy loss functions; for the low and high values of the excitation spectrum we have used the experimental energy loss functions ([16] for carbon and [17] for aluminum) and the X-ray scattering factors [18], respectively. The inclusion of the higher excitation energies in our description has a minor contribution to the self-retarding force and is negligible in the wake force. In Fig. 1 we depict the electric field induced by a proton moving with velocity $v = 5$ a.u. through amorphous carbon or aluminum; z and ρ are the coordinates relative to the position of the proton, parallel and perpendicular, respectively, to its velocity. The self-retarding force is obtained from the electric field at the position of the proton, $(z, \rho) = (0, 0)$. The magnitude and direction of the interference force depend on the relative position of both protons. This force has a tendency to align the internuclear axis of both protons with the direction of motion; this effect is more pronounced in the backward direction and so the trailing proton is more affected by the interference force. For the projectile velocity represented in Fig. 1, the

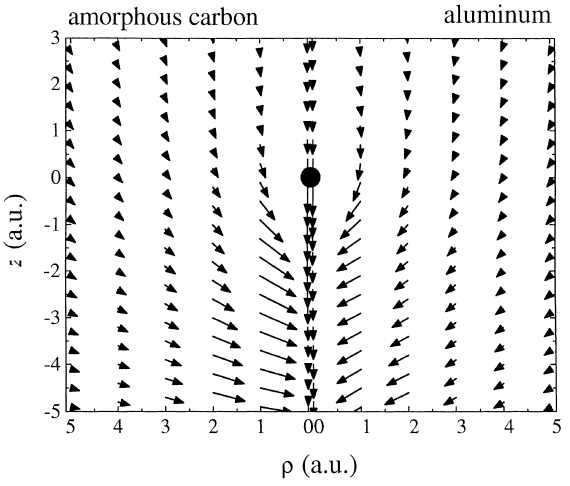

Fig. 1. Electric field induced in the medium by a proton moving with velocity $v = 5$ a.u. through an amorphous carbon or an aluminum target. The proton, indicated by a black circle at the coordinates $(z, \rho) = (0, 0)$, is moving in the positive z direction.

alignment tendency is larger in amorphous carbon than in aluminum.

The mutual repulsion of both protons was modeled with a Coulombic interaction and the nuclear collisions of the protons with the target atoms were incorporated through a Monte Carlo model [19], where the universal potential cross-section [20] was used to calculate the scattering angles and the corresponding nuclear energy loss. The effect of the coherent scattering [21,22] is taken into account with an effective force model. In this model [21], the coherent scattering is replaced by a force that only depends on the perpendicular component ρ of the internuclear separation, which tends to align the internuclear vector with the velocity and has the approximate form

$$F_{\mathrm{coh}}(\rho) = -\pi N Z_2 \cdot \begin{cases} \rho & \text{if } \rho \leqslant 2\rho_{\min}, \\ 4\rho_{\min}^2/\rho & \text{if } \rho \geqslant 2\rho_{\min}, \end{cases} \qquad (1)$$

where Z_2 is the atomic number of the target atoms, N the target atomic density and $\rho_{\min}$ a quantity depending on the velocity of the projectile and the target thickness, defined in [21].

Finally, after the protons leave the target, we calculate their asymptotic velocities and coordinates as a result of a pure Coulomb repulsion in the vacuum until they arrive at the detector.

3. Results

The possibility to incorporate or remove in our simulations each one of the interactions mentioned in the previous section helps to understand their different effects in the exit angle and energy loss distributions. In Fig. 2 we show the joint distribution of exit angle and energy loss of the fragment protons resulting from a H_2^+ ion incident with velocity $v = 5$ a.u. on a 150 a.u.-thick amorphous carbon or aluminum target. In the following, a label without (with) a prime corresponds to an amorphous carbon (aluminum) target. The contribution of the Coulomb explosion is represented in Fig. 2(a), and it is identical for both targets. In Fig. 2(b) and (b′) we have also added the interference effects due to the electronic excitations (wake forces) induced in the solid by the partner proton. The effect of the nuclear collisions was incorporated in Fig. 2(c) and (c′). The coherent scattering is included in Fig. 2(d) and (d′) and finally in Fig. 2(e) and (e′) we have added the contribution of the self-retarding force. These final pictures contain the contributions of all the interactions together.

The constant intensity and ring-shaped distribution of exit angle and energy loss (Fig. 2(a)) is typical of situations [8] in which there is only Coulomb explosion. Basically, the Coulomb explosion accelerates the leading proton and decelerates the trailing one; however, this effect is symmetric, and the energy gained by one proton is compensated by the energy lost by its partner, so that the mean energy loss is equal to zero.

The addition of the interference effects, seen in Fig. 2(b) and (b′), produces two asymmetrical peaks in the distribution at zero angle. These two peaks correspond to fragments of the H_2^+ molecule whose internuclear vector becomes aligned with the velocity direction. The higher peak comes from the trailing protons that were aligned by the wake force of the leading ones. Due to the asymmetry of the wake potential, this effect contributes to a minor extent to the alignment of the leading protons, which produce a lower peak. The mean energy loss in this case is not zero due mainly to the accumulation of trailing protons at zero angle.

Fig. 2(c) and (c′) shows a broadening of the angular distribution and a partial frustration of the previous alignment tendency, which is caused by the additional inclusion of the nuclear scattering processes. The difference between the intensity of the two peaks at zero angle diminishes, and the mean energy loss at zero angle is reduced compared with Fig. 2(b) and (b′). The inclusion of the coherent scattering in Fig. 2(d) and (d′) does not change very much the shape of the distributions. The force, F_{coh}, considered here for this effect tends to align the internuclear vector with the velocity and so it contributes to both peaks appearing at zero angle. However, for the cases considered here, this force is one order of magnitude lower than the wake force. Moreover, it may be shown that the coherence scattering effect is effective only for small values of ρ (nearly aligned particles). For

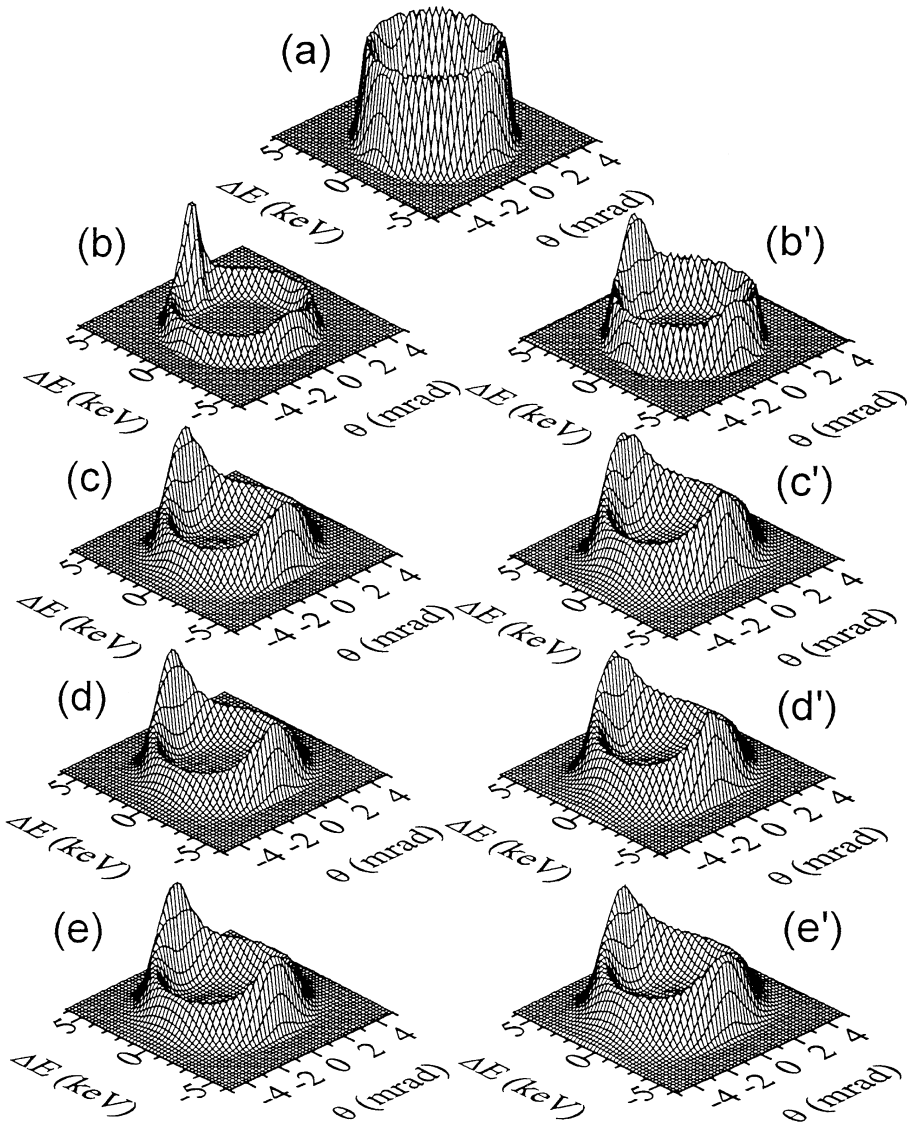

Fig. 2. Joint distribution of exit angle and energy loss of the protons resulting from the dissociation of H_2^+ molecular ions with $v = 5$ a.u. when traversing an amorphous carbon or an aluminum target, with thicknesses of 150 a.u. In (a) only the Coulomb explosion was considered. The following interactions were taken into account in the other cases: (b and b′) Coulomb explosion and interference effects; (c and c′) Coulomb explosion, interference effects and nuclear scattering; (d and d′) Coulomb explosion, interference effects, nuclear scattering and coherent scattering; (e and e′) all the interactions together, including the individual stopping power. A label without (with) a prime corresponds to an amorphous carbon (aluminum) target.

this reason the coherent scattering only represents a small perturbation to the major effect of the wake. The incorporation of the self-retarding force shown in Fig. 2(e) and (e′) only shifts the energy loss scale in a value equal to the energy loss of an individual proton, without changing the shape of the distribution.

We compare in Fig. 3 the energy loss distributions at zero angle, for amorphous and aluminum targets, in terms of the different interactions that

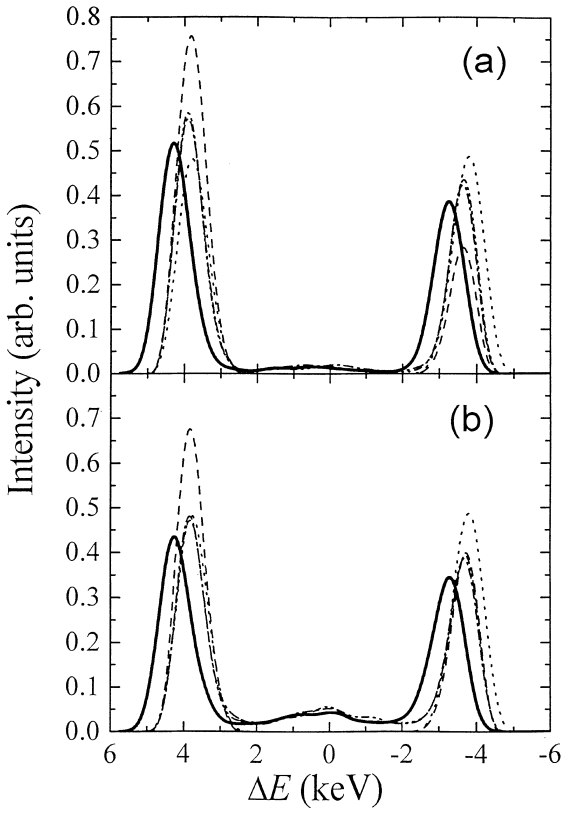

Fig. 3. Contributions of the different interactions to the energy loss distribution of protons at zero exit angle from a 150 a.u.-thick target bombarded with H_2^+ of $v = 5$ a.u. (a) amorphous carbon target and (b) aluminum target. Only Coulomb explosion is considered (···). Coulomb explosion and interference effects (– – –). Coulomb explosion, interference effects and nuclear scattering (– · –). Coulomb explosion, interference effects, nuclear scattering and coherent scattering (– · ·–). All the interactions together: Coulomb explosion, interference effects, nuclear scattering, coherent scattering and self-retarding force (—).

participate during the passage of the protons through the solid. The results shown correspond to the case of a $v = 5$ a.u. H_2^+ ion beam bombarding a 150 a.u.-thick foil. Coulomb explosion gives the same symmetric spectrum for carbon and aluminum. This symmetry is broken by the inclusion of the interference force and two asymmetrical peaks appear corresponding to the leading and trailing protons. This difference between the peaks is more pronounced in amorphous carbon because the electric field induced by a proton in this material has a greater tendency than in aluminum to align the internuclear axis with the velocity. The inclusion of the nuclear scattering reduces the asymmetry between both peaks. This effect is more pronounced in aluminum due to the stronger interatomic force of these atoms compared with the carbon atoms. Also nuclear scattering allows a fraction of particles to appear at zero angle and with very small ΔE producing a small central peak, which is more noticeable in aluminum. The inclusion of the coherent scattering enlarges both peaks but this is a rather small effect. Finally a net energy shift is produced by the inclusion of the self-retarding force and also a small broadening of the peaks due to the electronic energy loss straggling. This shift in energy loss is almost the same in carbon and aluminum because the stopping power at the velocity we are discussing practically coincides for both materials [4].

Fig. 4 shows the mean energy loss of the proton fragments, normalized to the mean energy loss at zero angle, as a function of their exit angle. The results correspond to the cases of three different projectile velocities ($v = 1$, 2 and 5 a.u.) and two different targets (amorphous carbon and aluminum) with the same thickness of 150 a.u. The mean energy loss as a function of the exit angle shows

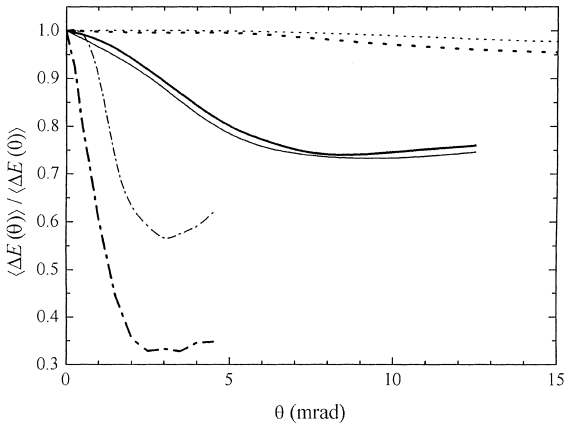

Fig. 4. Mean energy loss as a function of the exit angle, of the protons resulting from the dissociation of a H_2^+ ion in amorphous carbon (thick lines) and aluminum (thin lines) targets of 150 a.u. thickness: $v = 1$ a.u. (···), $v = 2$ a.u. (—) and $v = 5$ a.u. (– · –). The energy loss axis is normalized with the energy loss at zero exit angle.

the same trends for both targets. For all the velocities analyzed, it decreases with the angle until it reaches a minimum. The explanation lies in the number of trailing protons accumulated at zero angle, which displaces the mean energy loss towards the trailing peak. The growth of the mean energy loss with the exit angle, after the minimum value is reached, can be understood by the increase in the effective pathlength travelled by the protons. When the projectile velocity decreases, our calculations tend to the same behavior than recent results [23] reporting that the mean energy loss of the fragment protons increases with the exit angle, which is what should be expected for large dwell times (as is the case in Ref. [23]). Our results show that for short dwell times (when the internuclear separation is not very large) the wake effects are important in the mean energy loss of the fragment protons as a function of the exit angle, but these effects are negligible for large dwell times due to the path length increase for the more and more separated fragments.

The evolution of the internuclear distance distribution corresponding to pairs of protons at the exit of the amorphous carbon and aluminum foils is shown in Fig. 5 for several incident velocities and foil thicknesses. As a general trend, it is observed that the proportion of internuclear

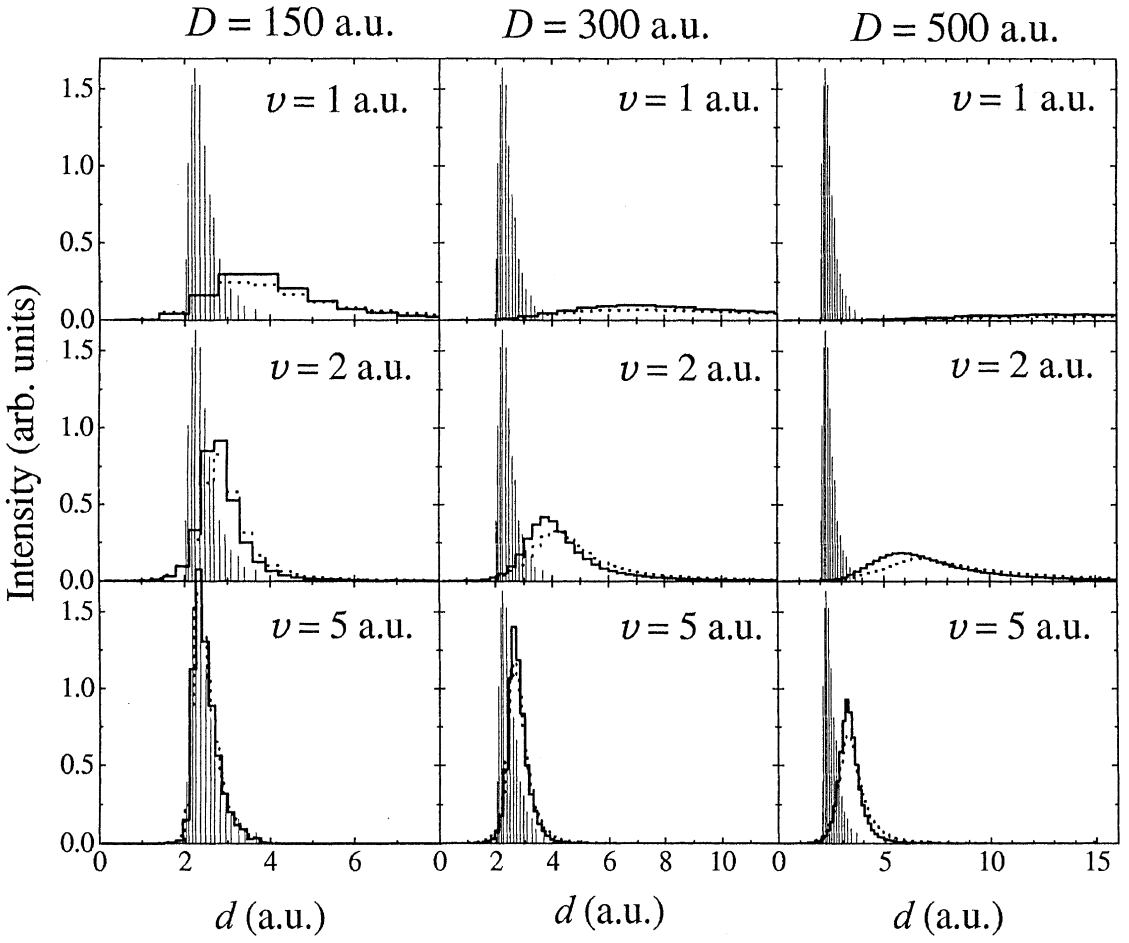

Fig. 5. Internuclear distance distributions of the fragment protons at the exit of an amorphous carbon (—) or aluminum (···) target, for the thicknesses and velocities indicated in the figure. The thin bars represent the initial internuclear distance distribution.

distances that falls within the initial distribution (indicated by a histogram with thin bars) is larger for the thinner foils and for the faster beams, because in these cases the dwell time is small enough and the proton fragments have almost no time to modify their relative positions. As the dwell time increases (for slower projectiles or thicker targets) the distribution of internuclear separations broadens and only a small portion of distances coincides with the initial distribution. Assuming that the transmission probability of the H_2^+ molecule is proportional to the intersection between the initial and final distributions of internuclear distances, we find a qualitative agreement with previous experimental results for the transmitted fraction of molecular ions [7], although more detailed predictions should involve the distribution of relative velocities and the electron capture probability at the exit. In general, the internuclear distance distributions are similar for carbon and aluminum targets. The larger pathlengths travelled by the protons in aluminum, due to the nuclear scattering, permits internuclear separations that are slightly larger in this material.

4. Summary and conclusions

We have performed computer simulations of the distributions in exit angle, energy loss and internuclear distances of the protons dissociated from fast H_2^+ molecular ions, when they move through amorphous carbon and aluminum foils. The trajectory of each proton has been calculated solving numerically the corresponding equation of motion, taking into account the following interactions: (i) the Coulomb explosion between both protons; (ii) the interference effects due to the electronic excitation induced in the material by the partner proton; (iii) the nuclear collisions with the target nuclei; (iv) the coherent scattering, and (v) the self-retarding force.

The results we have obtained have been interpreted in terms of the different contributions of the above mentioned interactions. The distinct characteristics of the targets (amorphous carbon and aluminum) allows to understand the different behavior of the calculated distributions for both materials.

Acknowledgements

This work has been supported by the Spanish Dirección General de Enseñanza (project PB96-1118) and the Generalitat Valenciana (project GV99-54-1-01). CDD thanks the Fundación Séneca (Comunidad Autónoma de la Región de Murcia) for economical support during his stay at the Universidad de Murcia and the Argentinian CONICET for a posdoctoral fellowship.

References

[1] W. Brandt, A. Ratkowski, R.H. Ritchie, Phys. Rev. Lett. 33 (1974) 1325.
[2] D.S. Gemmell, J. Remillieux, J.C. Poizat, M.J. Gaillard, R.E. Holland, Z. Vager, Phys. Rev. Lett. 34 (1975) 1420.
[3] P.M. Echenique, R.H. Ritchie, W. Brandt, Phys. Rev. B 20 (1979) 2567.
[4] I. Abril, R. Garcia-Molina, C.D. Denton, F.J. Pérez-Pérez, N.R. Arista, Phys. Rev. A 58 (1998) 357.
[5] W. Brandt, R. Laubert, A. Ratkowski, Nucl. Instr. and Meth. 132 (1976) 57.
[6] Z. Vager, D.S. Gemmell, Phys. Rev. Lett. 37 (1976) 1352.
[7] J. Remillieux, Nucl. Instr. and Meth. 170 (1980) 31.
[8] D.S. Gemmell, Chem. Rev. 80 (1980) 301.
[9] Y. Horino, M. Renda, K. Morita, Nucl. Instr. and Meth. B 33 (1988) 178.
[10] A. Arnau, P.M. Echenique, R.H. Ritchie, Nucl. Instr. and Meth. B 40/41 (1989) 329.
[11] E. Ray, R. Kirsch, H.H. Mikkelsen, J.C. Poizat, J. Remillieux, Nucl. Instr. and Meth. B 69 (1992) 133.
[12] W.L. Walters, D.G. Costello, J.G. Skofronick, D.W. Palmer, W.E. Kane, R.G. Herb, Phys. Rev. 125 (1962) 2012.
[13] J. Remillieux, in: O.F. Nygaard, H.I. Adler, W.K. Sinclair (Eds.), Radiation Research: Biomedical, Chemical and Physical Perspectives, Proceedings of the Fifth International Congr. Rad. Res., Academic Press, New York, 1975.
[14] D.J. Planes, R. Garcia-Molina, I. Abril, N.R. Arista, J. Electr. Spectrosc. Relat. Phenom. 82 (1996) 23.
[15] N.D. Mermin, Phys. Rev. B 1 (1970) 2362.
[16] J. Cazaux, P. Gramari, J. Phys. (France) 38 (1977) L133.
[17] H.-J. Hagemann, E. Gudat, C. Kunz, Optical constants from the far infrared to the X-ray region: Mg, Al, Cu, Ag, Au, Bi, C, and Al_2O_3 (Deutsches Elecktronen-Synchroton Report DESY SR-74/7, Hamburg, 1974) (unpublished); J. Opt. Soc. Am. 65 (1975) 742.
[18] B.L. Henke, E.M. Gullikson, J.C. Davis, At. Data Nucl. Data Tabl. 54 (1993) 2.

[19] W. Moller, G. Pospiech, G. Schrieder, Nucl. Instr. and Meth. 130 (1975) 265.
[20] J.F. Ziegler, J.P. Biersack, U. Littmark, The Stopping and Range of Ions in Solids, Vol. 1, Pergamon, New York, 1985.
[21] Y.V. Kononets, Nucl. Instr. and Meth. B 33 (1988) 174.
[22] P. Sigmund, Phys. Rev. A 46 (1992) 2596.
[23] M.M. Jakas, N.E. Capuj, Phys. Rev. A 54 (1996) 5031.